Molecular Crystals and Liquid Crystals Incorporating Nonlinear Optics

Publication details, including instructions for authors and subscription information:
http://www.tandfonline.com/loi/gmcl17

Landau Theory of Blue Phases

R. M. Hornreich [a] & S. Shtrikman [a b]

[a] Department of Electronics, Weizmann Institute of Science, 76100, Rehovot, Israel

[b] Department of Physics, University of California, San Diego, La Jolla, CA, 92093

Version of record first published: 03 Jan 2007.

To cite this article: R. M. Hornreich & S. Shtrikman (1988): Landau Theory of Blue Phases, Molecular Crystals and Liquid Crystals Incorporating Nonlinear Optics, 165:1, 183-211

To link to this article: http://dx.doi.org/10.1080/00268948808082201

Mol. Cryst. Liq. Cryst., 1988, Vol. 165, pp. 183–211
Reprints available directly from the publisher
Photocopying permitted by license only

Printed in the United States of America

Landau Theory of Blue Phases

R. M. HORNREICH and S. SHTRIKMAN†

Department of Electronics, Weizmann Institute of Science, 76100 Rehovot, Israel

(*Received December 23, 1987*)

The Landau theory of cholesteric blue phases (BP) is reviewed. The emphasis is on basic concepts, including (1) why BP appear between the disordered and ordinary helicoidal phases at sufficiently short pitch, and (2) why there are several cholesteric BP with different structures. These and other results in agreement with experimental findings are shown to follow from a simple theoretical model with *no* free parameters. Several examples of how calculations are carried out in practice are given.

I. INTRODUCTION

The theoretical description of the blue phases (BP) occurring in cholesteric liquid crystals has been one of the outstanding successes of the Landau theory of phase transitions. By analyzing a conceptually simple model functional for the free energy with *no* free parameters, a *universal phase diagram* including the two experimentally observed cubic BP as well as the high-temperature disordered and low-temperature helicoidal phases has been obtained.[1–3] In addition, the Landau model has been extended to include the effect of an external field on the phase diagram. This led to the prediction of a stable hexagonal structure in a region of the extended thermodynamic phase space[4]; a prediction which has since been confirmed experimentally.[5]

Our objective here is to give an overview of the Landau theory approach to cholesteric BP. We begin with a brief summary of the salient experimental results.[6] Many of these will be found to flow naturally from the Landau model analysis. Next, we introduce the Landau theory of cholesteric liquid crystals, emphasizing particularly how it explains why complex phases *must* appear between the dis-

†Also with the Department of Physics, University of California, San Diego, La Jolla, CA 92093.

ordered (isotropic) phase and the usual cholesteric (helicoidal) one when the cholesteric pitch is sufficiently short.[1] We then consider possible structures for these new phases, as obtained from the Landau theory analysis. Following the development of the theoretical concepts and models, we conclude by indicating where further theoretical studies could assist in resolving open questions.

II. The Cholesteric Blue Phases

Although they were first observed a century ago, it is only during the past decade that the properties of the anomalous phases which appear in many cholesteric liquid crystal systems immediately below their clearing point have been extensively investigated both experimentally and theoretically. Experimentally, the following have been established[6];

(1) The BP appear only when the usual cholesteric (helicoidal) phase has a "short" pitch. That is, when the pitch is increased (by, e.g., mixing different materials) the BP temperatue range always narrows and, eventually, disappears. This is illustrated in Figure 1.

(2) The BP region is narrow, generally being 1–2 K.

(3) The BP regime consists, as shown in Figure 1, of up to *three* distinct thermodynamic phases. The BPII region apparently disappears for very short cholesteric pitch.[7]

(4) All three BP are strongly optically active and non-birefringent.

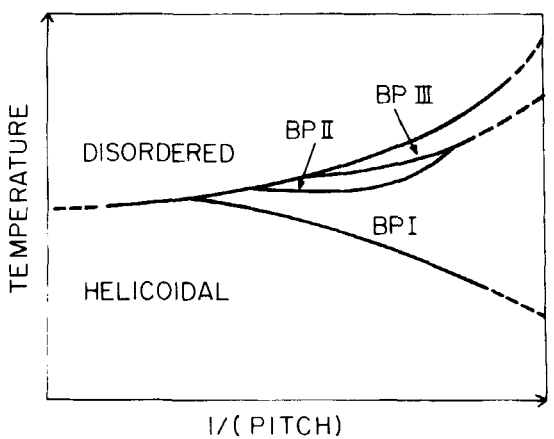

FIGURE 1 Schematic phase diagram, showing the three experimentally observed blue phases (BP).

(5) BPI and BPII both exhibit sharp Bragg peaks. Based on these and other (particularly, morphological) observations, it has been established that the former has a body-centered (*bcc*) and the latter a simple cubic (*sc*) structure. Note that this order is *orientational*, not translational; mechanically, these phases are liquids.

(6) BPIII, on the other hand, apparently does not exhibit Bragg scattering although a single, relatively broad, peak has been reported by Demikhov *et al.*[8]

(7) The latent heat peak on the disordered-BP phase boundary is an order-of-magnitude larger than those between BP's.[9] This indicates that locally all three BP and the cholesteric phase have essentially the same degree of order.

(8) Large (10–100 μ) single crystals of BPI and BPII with well-defined facets have been grown successfully in the BPI-disordered and BPII-disordered coexistence regions, respectively.[6,10] No crystallites of any size have been reported for BPII.

(9) In an applied field, at least *three additional phases* become thermodynamically stable. Bragg reflections and morphological studies[5] show that, in order of increasing field strength, these phases have a body-centered tetragonal and two different hexagonal structures. The latter differ in the presence or absence of a Bragg reflection parallel to the hexagonal axis; that is, they belong to three- and two-dimensional space groups, respectively.

III. FORMULATION OF THE LANDAU THEORY OF CHOLESTERICS

In the Landau theory of phase transitions,[11] one begins by choosing an appropriate *order parameter*. This time averaged quantity *vanishes* in the higher symmetry phase and become non-zero in the lower symmetry one. For example, to describe the liquid–solid transition, a convenient choice is $\Delta\rho(\mathbf{r})$, the deviation of the density $\rho(\mathbf{r})$ from its spatial average. This *scalar* quantity is zero in the liquid state and has non-zero Fourier amplitudes at points characteristic of the reciprocal lattice in the solid phase.

Another well-known example is the ferromagnetic phase transition. Here the order parameter is the magnetization $\mathbf{m}(\mathbf{r})$, which vanishes in the non-magnetic state. This particular order parameter is a *vector* quantity.

For many liquid crystal systems, on the other hand, neither a scalar or vector order parameter suffices since ordinary thermotropic liquid

crystals are composed of rod-like molecules.[12] These systems exhibit orientational (*not* translational) order below a critical temperature. Macroscopically, this order evidences itself as an anisotropy in the system's second-order tensor properties (e.g., the dielectric or diamagnetic tensor). A *tensor* can thus be an appropriate order parameter. More specifically, in analogy with the scalar case, we shall take as our order parameter the anisotropic part of the dielectric tensor[1]

$$\epsilon_{ij}(\mathbf{r}) \equiv \epsilon_{ij}^{d}(\mathbf{r}) - \frac{1}{3}Tr(\epsilon^{d})\delta_{ij}. \tag{3.1}$$

By construction, this symmetric traceless quantity vanishes in the disordered phase where ϵ^d is isotropic and becomes non-zero in any phase characterized by orientational order of rod-like molecules.

In the nematic (N) liquid crystal phase, the rod-like molecules order spontaneously along a common axis. In this case, the expansion of the average Landau free energy density F_N in terms of $\epsilon_{ij}(\mathbf{r})$ has as its lowest order terms[12]

$$F_N = V^{-1}\int d\mathbf{r}\left[\frac{1}{2}\left(a\epsilon_{ij}^2 + c_1\epsilon_{ij,l}^2 + c_2\epsilon_{ij,i}^2\right) - \beta\epsilon_{ij}\epsilon_{jl}\epsilon_{li} + \gamma(\epsilon_{ij}^2)^2 - \frac{1}{8\pi}\epsilon_{ij}E_iE_j\right], \tag{3.2}$$

where we have included explicitly in F_N *all* symmetry-allowed terms to fourth-order in ϵ_{ij} itself and to second-order in ϵ_{ij} and its spatial derivatives. The notation in Eq. (3.2) is as follows: a is proportional to a reduced temperature, β, γ, c_1, and c_2 are temperature-independent parameters, V is volume, $\epsilon_{ij,l} \equiv \partial\epsilon_{ij}/\partial r_l$, $\mathbf{E}$ is an applied field, and we sum on all repeated indices. For thermodynamic stability (i.e., the requirement that F_N be positive for sufficiently large values of the order parameter and its derivatives) both γ and c_1 must be positive. We shall see shortly that, in addition, it is necessary that c_2 be greater than $-(3/2)\,c_1$. There is only *one* fourth-order invariant in Eq. (3.2) as

$$(\epsilon_{ij}^2)^2 = 2\epsilon_{ij}\epsilon_{jl}\epsilon_{ln}\epsilon_{ni}, \tag{3.3}$$

for any rank two symmetric traceless tensor of dimension three.

More interesting is the case of *cholesteric* (C) liquid crystals. Here, the rod-like molecules are *chiral*; that is, they have a characteristic right- or left-handed twist which results in optically active ordered

phases. This chiral property is reflected in the existence in the Landau free energy of an additional invariant, giving[12]

$$F_C = V^{-1} \int d\mathbf{r} \left[\frac{1}{2} (a\epsilon_{ij}^2 - 2de_{ijl}\epsilon_{in}\epsilon_{jn,l} + c_1\epsilon_{ij,l}^2 + c_2\epsilon_{ij,i}^2) \right.$$

$$\left. - \beta\epsilon_{ij}\epsilon_{jl}\epsilon_{li} + \gamma(\epsilon_{ij}^2)^2 - \frac{1}{8\pi}\epsilon_{ij}E_iE_j \right]. \quad (3.4)$$

Here d is an additional temperature-independent parameter and e_{ijl} is the usual antisymmetric third-order tensor. The sign of d is fixed by the handedness of the chiral molecules; we shall take it to be positive.

It will be convenient in the following to introduce the following scaled quantities[1,2]:

$$\mu_{ij} = \epsilon_{ij}/(\beta/\sqrt{6}\gamma), \quad f = F_C/(\beta^4/36\gamma^3), \quad \frac{1}{4}t = (3\gamma/\beta^2)a,$$

$$\frac{1}{4}\xi_R^2 = (3\gamma/\beta^2)c_1, \quad c_2/c_1 = \rho, \quad \kappa = (d/c_1)\xi_R = q_C\xi_R, \quad (3.5)$$

$$\mathbf{x} = \mathbf{r}/\xi_R, \quad \mu_{ij,l} = \mu_{ij}/\partial x_l, \quad v = V/\xi_R^3, \quad \mathbf{e} = \mathbf{E}/(4\pi\beta^3/3\gamma^2)^{1/2}.$$

Equation (3.4) then becomes

$$f = v^{-1} \int d\mathbf{x} \left[\frac{1}{4}(t\mu_{ij}^2 - 2\kappa e_{ijl}\mu_{in}\mu_{jn,l} + \mu_{ij,l}^2 + \rho\mu_{ij,i}^2) \right.$$

$$\left. - \sqrt{6}\mu_{ij}\mu_{jl}\mu_{li} + (\mu_{ij}^2)^2 - \sqrt{6}\mu_{ij}e_ie_j \right]. \quad (3.6)$$

Note particularly that the pitch-temperature-field or (κ, t, $\mathbf{e}$) phase diagram obtained by minimizing f can depend upon only a single parameter, ρ.

Since we shall be interested in periodic (for BPIII, quasiperiodic) structures, we expand $\mu_{ij}(\mathbf{x})$ in Fourier components[1-3]

$$\mu_{ij}(\mathbf{x}) = \sum_{\sigma,n} N^{-\frac{1}{2}}(\sigma)\mu_{ij}(\sigma,n)\exp(i\mathbf{q}_{\sigma,n}\cdot\mathbf{x}), \quad (3.7a)$$

$$= \sum_{h,k,l} N^{-\frac{1}{2}}(\sigma)\mu_{ij}(h,k,l)\exp[iq(hx_1 + kx_2 + lx_3)]. \quad (3.7b)$$

In Eq. (3.7*a*) $n = -N(\sigma)/2, \ldots, -1, 1, \ldots, N(\sigma)/2$ runs over the set of $N(\sigma)$ wave vectors of magnitude $q_\sigma = |\mathbf{q}_{\sigma,n}| = \sigma^{1/2} q$ with $\mathbf{q}_{\sigma,-n} = -\mathbf{q}_{\sigma,n}$. The parameter σ (not necessarily integer) indexes wave vectors of different magnitudes. The alternate form, Eq. (3.7*b*), is particularly suited to the case of cubic structures; here (h,k,l) are Miller indices, $\sigma = h^2 + k^2 + l^2$, and $N(\sigma) = (3!)2^{3-n_0}/n_1!$ where $n_o(n_1)$ is the number of vanishing (equal) $|h|$, $|k|$, $|l|$ values for each distinct set $\{h,k,l\}$. The wave vector parameter q is dimensionless (*i.e.*, it is in units of ξ_R^{-1}) and is fixed by minimizing the free energy.

The tensors $[\mu_{ij}(\sigma,n)]$ or $[\mu_{ij}(h,k,l)]$ can each be expanded in terms of five basis tensors. For $[\mu_{ij}(\sigma,n)]$ we have

$$
\begin{aligned}
[\mu_{ij}(\sigma,n)] &= \sum_{m=-2}^{2} \mu_m(\sigma) e^{i\psi_m(\sigma,n)} [M_m(\sigma,n)] \\
&= \frac{1}{2}\Bigg[\mu_2 e^{i\psi_2} \begin{pmatrix} 1 & i & 0 \\ i & -1 & 0 \\ 0 & 0 & 0 \end{pmatrix} + \mu_1 e^{i\psi_1} \begin{pmatrix} 0 & 0 & 1 \\ 0 & 0 & i \\ 1 & i & 0 \end{pmatrix} \\
&\quad + \sqrt{\frac{2}{3}} \mu_0 e^{i\psi_0} \begin{pmatrix} -1 & 0 & 0 \\ 0 & -1 & 0 \\ 0 & 0 & 2 \end{pmatrix} \\
&\quad + \mu_{-1} e^{i\psi_{-1}} \begin{pmatrix} 0 & 0 & -1 \\ 0 & 0 & i \\ -1 & i & 0 \end{pmatrix} + \mu_{-2} e^{i\psi_{-2}} \begin{pmatrix} 1 & -i & 0 \\ -i & -1 & 0 \\ 0 & 0 & 0 \end{pmatrix} \Bigg]
\end{aligned}
\tag{3.8}
$$

Here $\mu_m(\sigma) \geq 0$ and we have suppressed the indices (σ,n) on μ_m and ψ_m in the final expression. The basis matrices are defined in a local right-handed coordinate system $(\hat{\xi},\hat{\eta},\hat{\zeta})$ for each (σ,n) with the polar axis $\hat{\zeta} \equiv \hat{q}_{\sigma,n}$. The directions of the other two axes are reflected in the choice of phases $\psi_m(\sigma,n)$. Requiring that $\hat{\xi}(\sigma,n) = \hat{\xi}(\sigma,-n)$ and $\hat{\eta}(\sigma,n) = -\hat{\eta}(\sigma,-n)$ results in $\psi_m(\sigma,n) = -\psi_m(\sigma,-n)$. Note that the basis matrices satisfy the orthogonality condition

$$
(M_m)_{ij}(M_{m'})_{ij} = \delta_{m(-m')}. \tag{3.9}
$$

For cubic structures, the indices (σ,n) in Eq. (3.8) are replaced by (h,k,l) and $\hat{\zeta} \equiv (h\hat{x}_1 + k\hat{x}_2 + l\hat{x}_3)/\sigma^{1/2}$.

Using Eqs. (3.7) and (3.8), the calculation of the quadratic part f_2 of f is straightforward. The result is

$$f_2 = \frac{1}{4}\sum_{\sigma,m}\{t - \kappa m q \sigma^{1/2} + [1 + \frac{1}{6}\rho(4 - m^2)q^2\sigma\}\mu_m^2(\sigma). \quad (3.10)$$

Since, in Landau theory, the explicit q-dependence of f appears only in f_2, we have $\partial f/\partial q = \partial f_2/\partial q = 0$, and

$$q = \frac{1}{2}\kappa\left\{\sum_{\sigma,m}[m\sigma^{1/2}\mu_m^2(\sigma)]\right\}\Bigg/\left\{\sum_{\sigma,m}\left[1 + \frac{1}{6}\rho(4 - m^2)\right]\sigma\mu_m^2(\sigma)\right\}. \quad (3.11)$$

For cubic structures particularly, a more convenient quantity is[1,2]

$$r \equiv \sqrt{2}q/\kappa = (q\xi_R^{-1})/(q_C/\sqrt{2}). \quad (3.12)$$

Of course, any $h = k = l = \sigma = 0$ term (if included in Eq. (3.10)) is excluded from the sums in Eq. (3.11).

To summarize, the scaled average Landau free energy density of cholesterics has the form

$$f = \frac{1}{4}\sum_{\sigma,m}\left\{t - \kappa m q\sigma^{1/2} + \left[1 + \frac{1}{6}\rho(4 - m^2)\right]q^2\sigma\right\}\mu_m^2(\sigma) + v^{-1}\int d\mathbf{x}[-\sqrt{6}\mu_{ij}\mu_{jl}\mu_{li} + (\mu_{ij}^2)^2 - \sqrt{6}\mu_{ij}e_ie_j], \quad (3.13)$$

with q determined implicitly via Eq. (3.11). Our objective is to minimize the free energy functional $f([\mu])$ at an arbitrary point in the $(\kappa,t,\mathbf{e})$-space. As noted earlier, there is only a single parameter (ρ) in the free energy expression. We shall consider here the case $\mathbf{e} = 0$, possible $\mathbf{e} \neq 0$ structures will be reviewed elsewhere.[13]

IV. FREE ENERGY CALCULATIONS

A. General Considerations

The primary ingredient of all ordered cholesteric phases can be understood by considering the lowest order (quadratic) part of the Landau free energy. For the special case of nonchiral (*i.e.*, racemic or R)

mixtures, $\kappa = 0$ and the transition is from the isotropic (I) phase to R, where $q = 0$. The excitation spectrum for this case is shown in Figure 2(a) for $\rho > 0$. Note (see Eq. (3.13)) that $1 + 2/3\rho > 0$ or, equivalently, $c_1 + (2/3)c_2 > 0$ is required for thermodynamic stability.

In the R or N phase, the free energy is minimized by a uniaxial

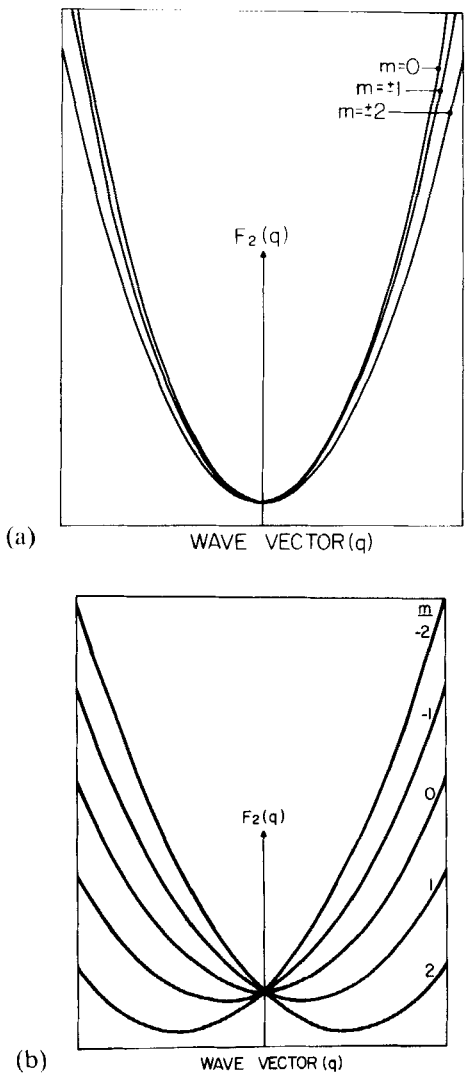

FIGURE 2 Wave vector (q) and eigenvalue (m) dependence of the quadratic part of the Landau free energy for: (a) a nematic liquid crystal or a racemic mixture, (b) a cholesteric liquid crystal.

and spatially uniform order parameter which may be taken in the form

$$\mu_{ij} = \frac{\mu}{\sqrt{6}} \begin{pmatrix} -1 & 0 & 0 \\ 0 & -1 & 0 \\ 0 & 0 & 2 \end{pmatrix}. \tag{4.1}$$

Then, for $\mathbf{e} = 0$,

$$f = f_R = \frac{1}{4} t\mu^2 - \mu^3 + \mu^4, \tag{4.2}$$

and the spontaneous I–R phase transition occurs at $t = t_R = 1$. Further, from Eq. (3.5), we see that the c_1-connected correlation length at $t = 1$ is just

$$\xi(t = 1) \equiv (c_1/a)_{t=1}^{1/2} = \xi_R. \tag{4.3}$$

Thus ξ_R is simply a correlation length (of a pure twist mode) for a racemic mixture on the I–R phase boundary and the unit of reduced temperature is the difference between the thermodynamic and extrapolated-from-the-disordered-phase transition temperatures for the same mixture.

Consider now the general case, $\kappa \neq 0$. The system is now chiral and the minimum of f_2 is necessarily at $q \neq 0$ (see Figure 2(b)). The thermodynamic stability requirement, $1 + (2/3)\rho > 0$, guarantees that the ground state will lie on the $m = 2$ branch of the spectrum. This branch is, in fact, the lowest-lying one for *all* σ provided that $\rho > 0$, a condition satisfied[12] by most liquid crystals near the order-disorder thermodynamic phase boundary. It follows that transverse $m = 2$ Fourier components are an essential ingredient in the structure of all ordered cholesteric phases.

The second key factor in the physics of cholesterics is that the transition from the I phase *cannot* be to the simple helicoidal cholesteric (C) structure for all values of κ. This can be understood as follows. Consider the *exact* form of the C-phase order parameter[1]

$$[\mu^C(\mathbf{x})] = -\frac{1}{\sqrt{6}}\mu_0 \begin{pmatrix} -1 & 0 & 0 \\ 0 & -1 & 0 \\ 0 & 0 & 2 \end{pmatrix} + \frac{1}{2\sqrt{2}}\mu_2 \left[\exp[i(\kappa z + \psi_2)] \begin{pmatrix} 1 & i & 0 \\ i & -1 & 0 \\ 0 & 0 & 0 \end{pmatrix} + cc \right], \tag{4.4}$$

where *cc* denotes complex conjugate. Substituting Eq. (4.4) into the free energy expression Eq. (3.13) with $\mathbf{e} = 0$ gives

$$f_C = \frac{1}{4} t\mu_0^2 + \frac{1}{4}(t - \kappa^2)\mu_2^2 + (\mu_0^3 - 3\mu_0\mu_2^2) + (\mu_0^2 + \mu_2^2)^2. \quad (4.5)$$

By minimizing f_C with respect to μ_0 and μ_2, for all κ, Grebel *et al.*[1] have shown that when $\kappa \geq 3$ an I–C phase transition, if it occurs, *must be of second-order* and take place at $t = t_{IC} = \kappa^2$. Rather than repeating their analysis, let us use a simpler approach. *If* the I–C phase transition is second-order for $\kappa \geq \kappa_0$, it is clear from Eq. (4.5) that (1) the transition occurs at $t = \kappa_0^2$, and (2) μ_2 is the primary and μ_0 a secondary order parameter proportional to μ_2^2 in this region. Setting $\mu_0 = \lambda\mu_2^2$, Eq. (4.5) becomes

$$f_C = \frac{1}{4}(t - \kappa^2)\mu_2^2 + (1 - 3\lambda + \frac{1}{4}t\lambda^2)\mu_2^4 + O(\mu_2^6). \quad (4.6a)$$

Minimizing f_C with respect to λ yields, to lowest order, $\lambda = 6/t$ and thus, as $t \to \kappa^2$, we have

$$f_c = \frac{1}{4}(t - \kappa^2)\mu_2^2 + (1 - 9/\kappa^2)\mu_2^4 + \ldots. \quad (4.6b)$$

To conform with our original assumption that the phase transition is second-order, it is necessary that the coefficient of μ_2^4 in Eq. (4.6*b*) be positive. This is met if and only if $\kappa \geq \kappa_0 = 3$.

Given this result, one may immediately ask whether a *first-order* transition from I to some ordered phase is possible for $\kappa \geq 3$. If so, such a transition *necessarily* occurs at a temperature $t > t_{IC}$ and the resulting ordered structure must have a free energy *lower* than that of either the I or C phases in some region of the (κ,t) phase diagram. A central objective of liquid crystal physics during the past decade has been to obtain a theoretical description of these new ordered structures and to compare their properties with those found experimentally for cholesteric BP.

Unfortunately, a global minimization of Eq. (3.13) at an arbitrary point in the (κ,t)-plane is extremely difficult. The approach taken[1–3] has therefore been to consider, individually, possible candidates for thermodynamically stable, non-helicoidal, cholesteric ordered phases. Since, as noted, we are interested in a first-order transition from the I phase, a key criterion in selecting candidates has been to require a non-zero third-order contribution to f. This naturally lead to the

consideration of structures with order parameters composed, at least in part, of Fourier components with $m = 2$ tensor amplitudes, each having an associated wave vector of (reduced) magnitude κ. The wave vector directions are chosen such that one or more equilateral triangles are formed, thereby giving the desired third-order contribution to f.

In the simplest three-dimensional structure satisfying this requirement, the wave vectors form a regular *tetrahedron*.[14] All the cubic phases analyzed in the literature ($O^5 - I432$, $O^8 - I4_132$, and $O^2 - P4_232$) take this tetrahedral "skeleton" as their starting point. Very recently, it has been suggested[15-17] that a structure based upon a skeleton formed by a regular *icosahedron* of wave vectors[18] could characterize BPIII. In order to compare the free energies of these alternate cubic and icosahedral structures, we must calculate the higher order terms in Eq. (3.13).

Generally speaking, two methods have been developed to evaluate these cubic and quartic contributions. In either, the first step is to express all the basis tensors in a common coordinate system. Next, in one approach, the closed loops formed by three or four wave vectors are identified and the contribution from each such loop is calculated by appropriate multiplication and tracing of the associated matrices.[1] Insofar as the phase factors are concerned, they may either be kept as free parameters to be fixed, together with the amplitudes, by free energy minimization or, better, determined *a priori* for each space group symmetry of interest. The actual matrix multiplication can be carried out by hand, in which case dyatic notation is particularly convenient, or by computer using a symbolic manipulator (e.g., REDUCE or MAXIMA).

In the alternate approach, all phase factors are first determined *ab initio* from the space group symmetry. Then all Fourier components whose associated wave vectors have a common length are combined and the result expressed as a real second-order matrix. The third- and fourth-order contributions to the free energy associated with each combination of the amplitudes are obtained by first multiplying and tracing the appropriate matrices and then extracting the trace's average value. While these steps can all be carried out analytically via symbolic manipulation, this approach is particularly suited to numerical implementation. For cubic structures, this has been done by calculating the matrix products and traces at representative points on a 3D net within a unit cell and then averaging by taking the arithmetic mean for each set of matrix products. For a reasonable number of points ($\sim 10^4$), six digit accuracy is attained.[2]

As already noted, it is the cubic term in the free energy which leads to thermodynamically stable non-helicoidal structures. A key "building block" is thus the third-order contribution from a single closed loop (*i.e.*, triangle) of wave vectors. In particular, we must consider contributions from triangles of wave vectors having $m = 2$ tensor amplitudes as these can minimize the quadratic part of the free energy.

Such a triangle is illustrated in Figure 3. In dyatic notation, the components of a basis tensor $[M_2]$ can be written as

$$[M_2]_{\alpha\beta} = u_\alpha u_\beta, \tag{4.7a}$$

with

$$\hat{u} \equiv (\hat{\xi} + i\hat{\eta})/\sqrt{2}. \tag{4.7b}$$

Here $\hat{\xi},\hat{\eta}$ are the real local unit vectors defined following Eq. (3.8).

We shall define a *canonical triangle* as one in which all three local $\hat{\xi}$ vectors are parallel and aligned with the normal to the triangle. The trace of the triple matrix product is then

$$\begin{aligned} T_3 \equiv [M_2(1)]_{\alpha\beta}[M_2(2)]_{\beta\gamma}[M_2(3)]_{\gamma\alpha} &= u_{1\alpha}u_{1\beta}u_{2\beta}u_{2\gamma}u_{3\gamma}u_{3\alpha} \\ = (\hat{u}_1 \cdot \hat{u}_2)(\hat{u}_2 \cdot \hat{u}_3)(\hat{u}_3 \cdot \hat{u}_1) &= \frac{1}{8}\prod_{\alpha=1}^{3}(1 + \cos\theta_\alpha), \end{aligned} \tag{4.8a}$$

where the θ_α are the vertex angles.

Suppose now that $\hat{\xi}_1$ is rotated about $\hat{q}_1$ *toward* $\hat{\eta}_1$ by an angle ϕ_1. Then $\hat{u}_1$ is replaced by $\hat{u}_1' = \hat{u}_1 e^{i\phi_1}$ and the trace becomes $T_3 e^{2i\phi_1}$.

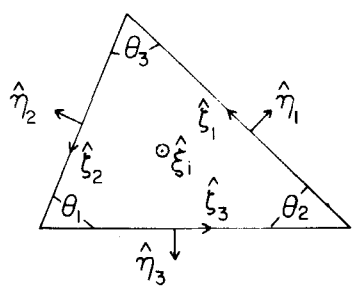

FIGURE 3 The canonical triangle contributing to the cubic term f_3 in the Landau free energy.

Thus, if all three $\hat{\xi}_\alpha$ are rotated through angles ϕ_α, the trace T_3 becomes

$$T_3' = \frac{1}{8} e^{2i(\phi_1 + \phi_2 + \phi_3)} \prod_{\alpha=1}^{3} (1 + \cos\theta_\alpha). \tag{4.8b}$$

This result will be basic to our analysis. Note that $Re(T_3') \leq T_3$ with the equality holding only when $\phi_1 + \phi_2 + \phi_3 = p\pi$ (p integer). Thus the magnitude of the third-order contribution to f will be maximum if all triangles are canonical.

B. The Tetrahedral Skeleton

The simplest three dimensional structure is obtained by choosing a set of wave vectors forming the six edges of a regular tetrahedron. From Figure 4 we see that the resulting structure is *bcc*. To minimize the quadratic part of the free energy, we associate with each of these wave vectors a single Fourier amplitude, composed (see Eq. (3.8)) of an $m = 2$ basis tensor, a phase factor and a common scalar magnitude. (The latter is a consequence of the (432) point group symmetry). The free energy is obviously minimized by taking the common (reduced) magnitude of the wave vectors equal to κ. We give in Table I the directions of the wave vectors and principal axes on each of the tetrahedron's edges. This set of wave vectors is labelled by $\sigma = 2$, $n = 1, \ldots, 6$.

Even before considering the phase angles $\psi_2(2,n)$, we can obtain

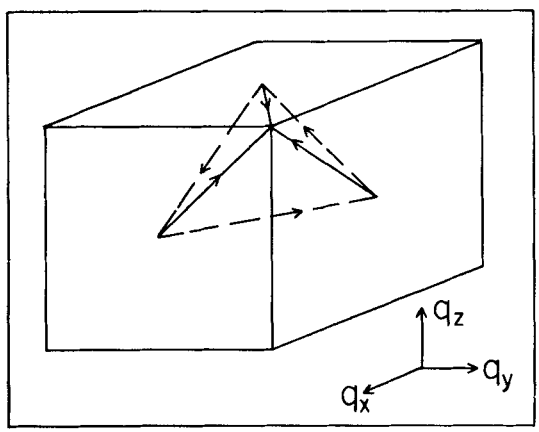

FIGURE 4 The tetrahedral skeleton structure. The set of six independent wave vectors are shown.

TABLE I

Wave vectors and local axis systems $(\hat{\xi},\hat{\eta},\hat{\zeta})$ for the $\langle 110 \rangle$ wave vectors illustrated in Figure 4. For the wave vectors $-\boldsymbol{\kappa}_{2,n}$, $\hat{\eta}_{2,n}$ is replaced by $-\hat{\eta}_{2,n}$. The wave vector parameter q is determined, in general, from Eq. (3.11).

Wave vector		
$(\boldsymbol{\kappa}_{2,n} = \sqrt{2}q\hat{\zeta}_{2,n})$	$\hat{\xi}_{2,n}$	$\hat{\eta}_{2,n}$
$\boldsymbol{\kappa}_{2,1} = \sqrt{2}q[(\hat{x} + \hat{y})/\sqrt{2}]$	$\hat{z}$	$(\hat{x} - \hat{y})/\sqrt{2}$
$\boldsymbol{\kappa}_{2,2} = \sqrt{2}q[(\hat{y} + \hat{z})/\sqrt{2}]$	$\hat{x}$	$(\hat{y} - \hat{z})/\sqrt{2}$
$\boldsymbol{\kappa}_{2,3} = \sqrt{2}q[(\hat{z} + \hat{x})/\sqrt{2}]$	$\hat{y}$	$(\hat{z} - \hat{x})/\sqrt{2}$
$\boldsymbol{\kappa}_{2,4} = \sqrt{2}q[(-\hat{x} + \hat{y})/\sqrt{2}]$	$-\hat{z}$	$-(\hat{x} + \hat{y})/\sqrt{2}$
$\boldsymbol{\kappa}_{2,5} = \sqrt{2}q[(-\hat{y} + \hat{z})/\sqrt{2}]$	$-\hat{x}$	$-(\hat{y} + \hat{z})/\sqrt{2}$
$\boldsymbol{\kappa}_{2,6} = \sqrt{2}q[(-\hat{z} + \hat{x})/\sqrt{2}]$	$-\hat{y}$	$-(\hat{z} + \hat{x})/\sqrt{2}$

the quadratic contribution to the average free energy as it is independent of these quantities. Since we have only $m = 2$ Fourier components, the ρ-dependent term in Eq. (3.13) vanishes. From Eq. (3.12), we have $q = \kappa$ and the quadratic part of f is just

$$f_2(2) = \frac{1}{4}(t - \kappa^2)\mu_2^2(2). \tag{4.9a}$$

To appreciate more clearly the essential elements of the free energy calculation, let us (temporarily) replace the quartic term in Eq. (3.13) by a simpler one

$$f_4 = v^{-1} \int d\mathbf{x}(\mu_{ij}^2)^2 \rightarrow f_4' = [v^{-1} \int d\mathbf{x}\mu_{ij}^2]^2. \tag{4.10}$$

This *modified quartic contribution* f_4' is also independent of the phases $\psi_2(2,n)$ and is just

$$f_4(2) \geq f_4'(2) = \mu_2^4(2), \tag{4.9b}$$

with $f_4 \geq f_4'$ following generally from the Schwartz inequality.

We turn now to the third-order contribution in Eq. (3.13). Here the phase angles play an important role. The optimum choice would clearly be to fix the phases such that each of the eight triangles (clockwise and counterclockwise) in Figure 4 contributes its canonical value which, from Eq. (4.8*a*), is (3/4).[3] This, however, is *impossible*. To see this, suppose that one of the clockwise triangles is in its canonical state. Since changing a given phase angle is equivalent to a rotation of the corresponding local $\hat{\xi},\hat{\eta}$ axes (by half the change), let us systematically rotate the local axes on the non-common legs of

neighboring clockwise triangles so that each gives a canonical contribution, *i.e.*, so that the sum $(\phi_1 + \phi_2 + \phi_3)$ *vanishes* for each. However, since the triangles form a closed surface, there will always be at least *one* clockwise triangle for which this sum cannot vanish. Thus the naive minimum value of f_3 *is unattainable for any choice of* $\psi_2(2,n)$. This is an example of *frustration*.

For cubic structures, it is straightforward to determine the phase angles (modulo π) *a priori* from the space group symmetry.[1,2] (For icosahedral structures the situation is more subtle).[15–17] As an example, consider the tetrahedral skeleton in Figure 4. Since $x = y = z$ can be taken as a three-fold axis for *all* cubic structures, we have immediately

$$\begin{aligned} \psi_2(2,1) &= \psi_2(2,2) = \psi_2(2,3); \\ \psi_2(2,4) &= \psi_2(2,5) = \psi_2(2,6). \end{aligned} \tag{4.11}$$

However, the physically relevant quantities are not the phase angles of individual edges but, rather, the phases associated with closed oriented loops. Since all such loops are ordered combinations of one or more triangles, it is sufficient to consider the phases ϕ_Δ associated with each of the equilateral triangles. From Figure 4 and Eq. (4.11), we find for the "explicit" phase ψ_Δ (*i.e.*, the algebraic sum of the $\psi_2(2,n)$ associated with the triangle's legs)

$$\begin{aligned} &\Delta(1,\bar{2},\bar{6}), \Delta(2,\bar{3},\bar{4}), \Delta(3,\bar{1},\bar{5}): \psi_{\Delta_a} = -\psi_2(2,4), \\ &\Delta(4,5,6): \psi_{\Delta_b} = 3\psi_2(2,4). \end{aligned} \tag{4.12}$$

Since ψ_{Δ_a} and ψ_{Δ_b} are independent of $\psi_2(2,1)$, it follows that this phase can always be set equal to 0 (or π). This is equivalent to choosing the point on the line $x = y = z$ at which we put our coordinate system origin.

We must now add to each ψ_Δ the "implicit" phase due to the angles between the local vectors $\hat{\xi}$ associated with each edge of a given triangle and the normal to that triangle. For the oriented loops in Figure 4, all the implicit phases are identical and, from Table I, are given by

$$\phi = -3 \arccos \frac{1}{3} \text{ (2nd quadrant)} = -\arccos (23/27). \tag{4.13}$$

Since ϕ is loop-independent, our system can have (432) point sym-

metry if and only if the implicit phases in Eq. (4.12) are all equal (modulo 2π). Equating these phases gives

$$\psi_2(2,4) = \pi p/2\ (+\pi), \tag{4.14a}$$

$$\phi_\Delta = \psi_\Delta + \phi = -\pi p/2 + \phi\ (+\pi). \tag{4.14b}$$

Here $p = 0,1$ and $(+\pi)$ indicates that $\psi_2(2,4)$ and ϕ_Δ can both be increased by π if this is necessary to make $f_3(2)$ negative.

For $|\phi_\Delta| < \pi/2$ (*i.e.*, a *negative* third-order term), there are thus *two* solutions to Eq. (4.12*b*). They are

$$\begin{aligned} p &= 0;\quad \phi_\Delta = \phi = -31.59°, \\ p &= 1;\quad \phi_\Delta = \pi/2 + \phi = 58.41°. \end{aligned} \tag{4.15}$$

There are thus two different skeleton structures compatible with (432) point symmetry. We shall label their respective free energies by the corresponding value of p. In general

$$f_3(2;p) = -[8\sqrt{6}(3/4)^3 3!/12\sqrt{12}] \cos(\phi + \pi p/2)\mu_2^3(2). \tag{4.16}$$

Since both skeleton structures have non-vanishing third-order contributions to f, it follows that *there must be one or more non-helicoidal phases in the phase diagram for sufficiently large* κ. This conclusion is *independent* of the actual structure of the new phase. We now determine which of the two possible skeleton structures is energetically preferred.

For the modified Landau free energy functional (with f_4 replaced by f_4'), the structure having the lowest free energy is that for which the coefficient of $\mu_2^3(2)$ in $|f_3|$ is maximum. From Eq. (4.15), this obviously occurs when $p = 0$; $f_3(2;0) = -1.020\mu_2^3(2)$. In principle, however, the ground state of the *bcc* skeleton structure could, for the unmodified Landau model, depend upon the value of f_4 (which, unlike f_4', *is* phase-dependent). We therefore turn to its evaluation.

The basic rule for obtaining a non-vanishing contribution to f_4 is identical to that for f_3; the wave vectors must form a closed polygon. Since four wave vectors are now involved, however, the polygon may be "degenerate," *i.e.*, may have the same wave vector occurring more than once, and also need not necessarily be planar. In general, there are three types of contributions, which can be calculated separately. They are[2]:

a) "Quadratic squared" contributions. These include all products of

traces having the form $Tr[M_2(2,n)M_2^*(2,n)]$. This is precisely the "modified" fourth-order term calculated earlier

$$[f_4(2)]_a = \frac{1}{(12)^2} 2^2 \mu_2^4(2) \left\{ \sum_{n=1}^{6} Tr[M_2(2,n)M_2^*(2,n)] \right\}^2 = \mu_2^4(2). \tag{4.17}$$

b) "Conjugate" contributions. Here the individual traces each have an associated wave vector and the two traces forming each product are complex conjugates. There are five products of this type, falling into two distinct sub-groups. The total contribution is

$$\begin{aligned}[f_4(2)]_b = \frac{1}{12^2}\left(\frac{6}{2}\right) 2^3 \mu_2^4(2) \{ & 4Tr[M_2(2,1)M_2(2,2)]Tr[M_2^*(2,1)M_2^*(2,2)] \\ & + 4Tr[M_2(2,1)M_2^*(2,2)]Tr[M_2^*(2,1)M_2(2,2)] \\ & + 4Tr[M_2(2,1)M_2(2,4)]Tr[M_2^*(2,1)M_2^*(2,4)] \\ & + 4Tr[M_2(2,1)M_2^*(2,4)]Tr[M_2^*(2,1)M_2(2,4)]\}.\end{aligned} \tag{4.18}$$

Note that both $(f_4)_a$ and $(f_4)_b$ are independent of the implicit and explicit phases; they are thus the same for both of the *bcc* skeleton structures. The evaluation of the terms in $(f_4)_b$ is straightforward since they, like $(f_4)_a$, are *independent* of our choice of local axes and phases. Consider the trace $Tr[M_2(2,n_1)M_2(2,n_2)]$ with $M_2(2,n_i) = u_{ni\alpha}u_{ni\beta}$ ($i = 1,2$). Take $\hat{u}_{n_1} = (\hat{\xi}_{n_1} + i\hat{\eta}_{n_1})/\sqrt{2}$, and $\hat{u}_{n_2} = (\hat{\xi}_{n_2} + i\hat{\eta}_{n_2})/\sqrt{2} = (\hat{\xi}_{n_1} \cos\theta_{n_1n_2} + i\hat{\eta}_{n_1})/\sqrt{2}$. Here $\theta_{n_1n_2}$ is the angle between the wave vectors $\boldsymbol{\kappa}_{2,n_1}$ and $\boldsymbol{\kappa}_{2,n_2}$ and we have chosen convenient local coordinate frames with $\hat{\eta}_{n_1} = \hat{\eta}_{n_2}$ along $\boldsymbol{\kappa}_{2,n_1} \times \boldsymbol{\kappa}_{2,n_2}$. We immediately have

$$Tr[M_2(2,n_1)M_2(2,n_2)] = (\hat{u}_1 \cdot \hat{u}_2)^2 = (1 - \cos\theta_{n_1n_2})^2/4. \tag{4.19a}$$

Thus

$$\begin{aligned}&Tr[M_2(2,n_1)M_2(2,n_2)Tr[M_2^*(2,n_1)M_2^*(2,n_2)] + \\ &Tr[M_2(2,n_1)M_2^*(2,n_2)]Tr[M_2^*(2,n_1)M_2(2,n_2)] = \\ &[(1 - \cos\theta_{n_1n_2})^4 + (1 + \cos\theta_{n_1n_2})^4]/16.\end{aligned} \tag{4.19b}$$

Since $\theta_{12} = 60°$ and $\theta_{14} = 90°$, we have from Eqs. (4.18) and (4.19*b*)

$$[f_4(2)]_b = \frac{15}{64}\mu_2^4(2). \tag{4.20}$$

c) "Loop" contributions. These come from the closed loops formed by summing four wave vectors with different n indices. Inspection of the tetrahedron in Figure 4 shows that there are eight such loops or, alternately, four clockwise and four counterclockwise ones. For our choice of local coordinate systems, these loop contributions to f_4 are all equal and we have

$$\begin{aligned}(f_4(2;p)]_c = \\ \frac{1}{(12)^2}(8)2^3\mu_2^4(2)Re\{&Tr[M_2(2,1)M_2^*(2,2)]Tr[M_2(2,4)M_2(2,5)] \\ &+ Tr[M_2(2,1)M_2(2,4)]Tr[M_2^*(2,2)M_2(2,5)] \\ &+ Tr[M_2(2,1)M_2(2,5)]Tr[M_2^*(2,2)M_2(2,4)]\}.\end{aligned} \tag{4.21}$$

This contribution, unlike $(f_4)_a$ or $(f_4)_b$, *is* structure-dependent. Using Table II, we obtain

$$\begin{aligned}[f(2;p)]_c &= \frac{1}{48}[1 + \left(\frac{81}{8}\right)cos(4\phi/3)]cos[2\psi_2(2,4)]\mu_2^4(2), \\ &= (25/384)(-1)^p.\end{aligned} \tag{4.22}$$

Summing Eqs. (4.17), (4.20), and (4.22), we have finally

$$f_4(2;p) = 79/64 + (25/384)(-1)^p. \tag{4.23}$$

Since the quadratic contribution $f_2(2)$ is structure-independent, the transition from the disordered to a *bcc* skeleton structure will occur at

$$t_{I-BCC}(2) = max(f_3^2/f_4) + \kappa^2. \tag{4.24a}$$

Clearly, from Eqs. (4.16) and (4.23), (f_3^2/f_4) is maximized when $p = 0$. In this case, the *bcc* skeleton structure is O^5 and we have

$$t_{IO^5}(2) = 1587/1966 + \kappa^2 = 0.795 + \kappa^2. \tag{4.24b}$$

TABLE II

Scalar products for the complex basis vectors $\hat{u}(2,n)) \equiv [\hat{\xi}(2,n)] + i\hat{\eta}(2,n)]/\sqrt{2}$ ($n = 1, \ldots, 6$). All other products can be found by cyclic permutation and complex conjugation. The angle ϕ is given in Eq. (4.13).

	$\hat{u}(2,1)$	$\hat{u}(2,2)$	$\hat{u}(2,4)$	$\hat{u}(2,5)$	$\hat{u}(2,6)$
$\hat{u}(2,1)$	0	$\frac{1}{4}$	$-\frac{1}{2}$	$\frac{3}{4}e^{-i\phi}$	$\frac{1}{4}$
$\hat{u}(2,4)$			0	$\frac{3}{4}e^{i\phi}$	
$\hat{u}^*(2,1)$	1	$\frac{3}{4}e^{-i\phi}$	$-\frac{1}{2}$	$\frac{1}{4}$	$\frac{3}{4}e^{-i\phi}$
$\hat{u}^*(2,4)$			1	$\frac{1}{4}$	

This result for t_{IO^5} should be compared with the comparable expression for t_{IC} which is[1]

$$t_{IC} = \frac{1}{2}[1 + \kappa^2 + (1 + \frac{1}{3}\kappa^2)^{\frac{3}{2}}], \text{ for } \kappa \leq 3,$$
$$= \kappa^2, \text{ for } \kappa > 3. \tag{4.25}$$

The result is that, for $\kappa \geq 0.939$, the I–O^5 transition occurs before (*i.e.*, at a *higher* temperature) than I–C. Upon solving also for the boundary between O^5 and C, the I–O^5–C phase diagram shown in Figure 5(a) is obtained.

C. The Role of Harmonics

In applying Landau theory to the cholesteric BP, it was quickly realized[19] that a model whose order parameter was restricted to a set of Fourier wave vectors having a *single* magnitude could not possibly describe the two experimentally observed cubic structures. In both cases, *harmonics* of the basic wave vector magnitude play a crucial role; they explain (1) why, experimentally, several Bragg reflections are observed, (2) why the primary reflection in both BPI and BPII does not appear at the same wavelength as that of the helicoidal phase, and (3) why *sc* O^2 and *bcc* O^8 have *lower* free energies that O^5 in regions of the (κ,t)-plane.

To systematically include harmonics in the Landau free energy, the first step is to determine the allowed spatial frequencies for a given structure. This is the analogue, in the optical wave band, of the

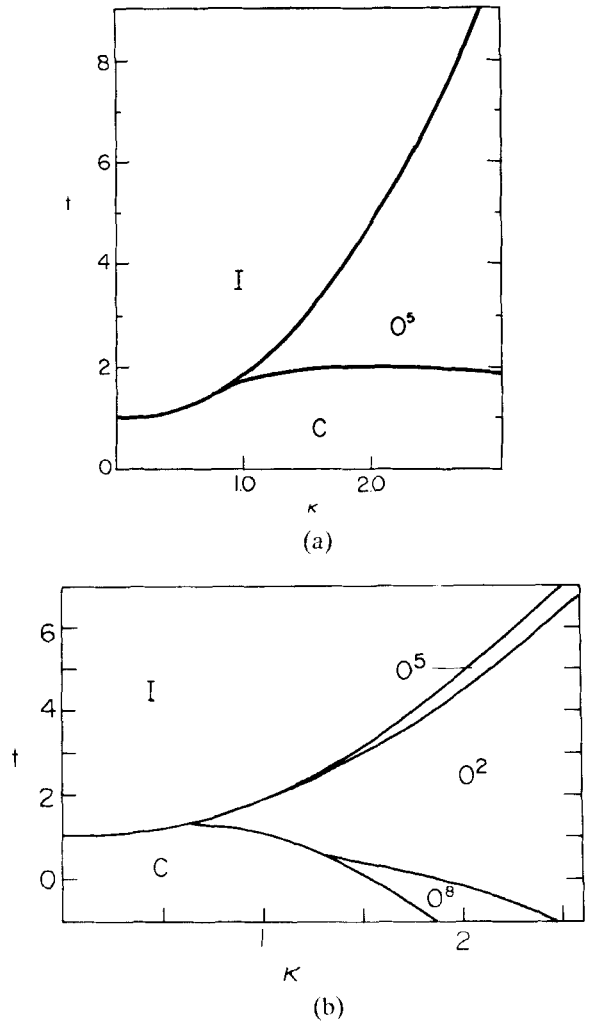

FIGURE 5 Theoretical phase diagram of cholesteric liquid crystals (from Ref. 2) when: (a) *only* disordered (I), cubic O^5, and helicoidal cholesteric (C) phases are allowed. (b) the disordered (I), cubic (O^2, O^5, O^8) and helicoidal cholesteric (C) phases are allowed.

structural factor commonly used in X-ray elastic scattering analysis. However, in our case, the BP structure factor has a tensor rather than scalar character as all elements of the order parameter can contribute to the scattering process.

A detailed explanation of how the BP tensorial structure factor is

obtained has been given elsewhere.[20] Results have been obtained[1,20] for all *bcc*, *sc*, (and also *fcc*[21]) space groups. We restrict ourselves here to the three cubic groups of immediate interest, *bcc* O^5 and O^8, and *sc* O^2 (see Table III). Note particularly that the selection rules given in this Table depend upon $[h,k,l;m]$. That is, for an allowed Bragg reflection $[h,k,l]$, the strength of the peak is dependent upon the polarization state of the incident radiation. Also, the Table entries are valid for *single* scattering events. Thus, in thick samples, where multiple scattering processes can contribute to observed peak intensities, they must be used cautiously.

From inspection of Table III, several conclusions can be quickly reached. Consider, for example, a back-scattering experiment using circularly polarized incident light. For O^5 symmetry, the ⟨200⟩ Bragg

TABLE III

Optical structure factor for *bcc* O^5 and O^8 and *sc* O^2. $S(W)$ denotes a strong (weak) Bragg reflection. X-ray selection rules are identical to those for $m = 0$.

$\frac{1}{2}(h^2 + k^2 + l^2)$	hkl	m:	(O^5)[a] 2	1	0	$\bar{1}$	$\bar{2}$		m:	(O^8)[b] 2	1	0	$\bar{1}$	$\bar{2}$	
1	110		+	−	+	−	+	S		+	−	+	−	+	S
2	200		−	−	+	−	−	W		+	−	−	−	+	S
3	211		+	+	+	+	+	S		+	+	+	+	+	S
4	220		+	−	+	−	+	S		+	−	+	−	+	S
5	310		+	+	+	+	+	S		+	+	+	+	+	S
6	222		−	−	+	−	−	W		−	−	+	−	−	W
7	321		+	+	+	+	+	S		+	+	+	+	+	S
8															
9	330		+	+	+	+	+	S		+	−	+	−	+	S

$(h^2 + k^2 + l^2)$	hkl	m:	(O^2)[c] 2	1	0	$\bar{1}$	$\bar{2}$	
1	100		+	−	−	−	+	S
2	110		+	−	+	−	+	S
3	111		−	−	+	−	−	W
4	200		−	−	+	−	−	W
5	210		+	+	+	+	+	S
6	211		+	+	+	+	+	S
7								
8	220		+	−	+	−	+	S
9	221		+	+	+	+	+	S

[a]Selection rules; $h + k + l = 2n$;$h00$: $m = 0$;$hh0$: $m = \pm 2,0$;hhh: $m = 0$.

[b]Selection rules; $h + k + l = 2n$;$h00$: $m = \pm 2, h = 4n - 2, m = 0, h = 4n$;$hh0$: $m = \pm 2,0$;hhh: $m = 0$.

[c]Selection rules. $h00$: $m = \pm 2$, $h = 2n - 1$, $m = 0, h = 2n$;$hh0$: $m = \pm 2,0$; hhh: $m = 0$.

peak is due to scattering from the $m = 0$ state only. *Thus it cannot be sensitive to the sense of the polarized light.* Moreover, this peak is associated with a relatively high-lying state and will necessarily be relatively *weak* in comparison with the ⟨110⟩ peak. For O^8 symmetry, on the other hand, the ⟨200⟩ Bragg peak has $m = \pm 2$ contributions. Since the $m = +2$ state is a low-lying one while $m = -2$ lies much higher, *this peak will be strongly sensitive to the sense of the incident radiation* and its intensity will be of the same order of magnitude as the primary ⟨110⟩ reflection. Turning to *sc* structures, we see that in all cases the *third* [here ⟨111⟩] *Bragg peak will be polarization independent and weak.* Thus we see that the selection rules in Table III provide, in principle, a direct and straightforward means of distinguishing among O^5, O^8, and O^2 structures which has been utilized experimentally.[6] In addition, they provide a framework within which a Landau theory calculation of the free energies appropriate to these structures can be carried out at any point in the (κ,t)-plane.

However, additional Fourier components in the order parameter make an analytic calculation of the third- and fourth-order terms in the Landau free energies a formidable task. As noted earlier, an alternate method, combining symmetry and numerical techniques, was therefore developed for cubic structures.[2] This approach allows one to systematically include the contributions of the additional harmonics. The procedure is as follows: First, the phases, $\psi_2(h,k,l)$ are determined (modulo π) *a priori* from the space group symmetry. Next, the coefficients of each of the third- and fourth-order terms in f are calculated numerically. This is done by constructing explicitly the real space matrix $\mu_{ij}(\mathbf{x},\sigma)$ for each value of σ included in the order parameter. The integrals in Eq. (3.13) are then divided into subsets having the form

$$I_3(\sigma_a,\sigma_b,\sigma_c) = -\sqrt{6}v^{-1}P\int \mathbf{d}x\mu_{ij}(\mathbf{x},\sigma_a)\mu_{jl}(\mathbf{x},\sigma_b)\,\mu_{li}(\mathbf{x},\sigma_c),$$

$$I_4(\sigma_a,\sigma_b,\sigma_c,\sigma_d) = v^{-1}P\int \mathbf{d}x\mu_{ij}(\mathbf{x},\sigma_a)\mu_{ij}(\mathbf{x},\sigma_b);_{ln}(\mathbf{x},\sigma_c)\mu_{ln}(\mathbf{x},\sigma_d). \tag{4.26}$$

The operator P permutes the σ_i in Eq. (4.26) such that all distinct permutations are included in each I_3 and I_4. Finally, the I_3 and I_4 integrals are evaluated numerically by sampling the unit cell (or a suitable part therefore) on a net of uniformly spaced points in the three-dimensional space. The number of sample points required is determined by comparing several of the computed integrals with analytically computed values. Six digit accuracy is easily obtained.

Consider first the *bcc* space group O^5. For all *bcc* groups σ must be *even*. For $m = 2$, we see from Table III that $\sigma = 4$ is *forbidden*, thus the lowest-lying Fourier components have $\sigma = 2$, 6, and 8. Setting our origin at the point (000) in the O^5 unit cell with point-group symmetry (432), it is straightforward to show that (a) this structure must have $p = 0$, (b) all $\sigma = 6$ phases are identical and equal to either 0 or π, and (c) the same holds for all $\psi_2(8,n)$.

Setting all phases equal to zero, the free energy is (with $\sigma = 2$, 6, and 8)[2]

$$\begin{aligned} F_{O^5} = \frac{1}{4}\sum_{\sigma}[t - \kappa^2 + \kappa^2(\sigma^{1/2}r/\sqrt{2} - 1)^2]\mu_2^2(\sigma) - 1.016\mu_2^3(2) \\ - 0.422\mu_2^3(6) \\ - 1.016\mu_2^3(8) - 1.306\mu_2^2(2)\mu_2(6) + 0.880\mu_2^2(6)\mu_2(8) \\ + 1.611\mu_2(2)\mu_2^2(6) \\ + 3.266\mu_2(2)\mu_2(6)\mu_2(8) + 1.299\mu_2^4(2) + 1.436\mu_2^4(6) \\ + 1.299\mu_2^4(8) \\ + 0.791\mu_2^3(2)\mu_2(6) - 0.656\mu_2^3(2)\mu_2(8) + 434\mu_2^3(6)\mu_2(8) \\ - 0.428\mu_2(2)\mu_2^3(6) \\ + 2.916\mu_2^2(2)\mu_2^2(6) + 2.891\mu_2^2(2)\mu_2^2(8) + 2.341\mu_2^2(6)\mu_2^2(8) \\ - 0.363\mu_2^2(2)\mu_2(6)\mu_2(8) - 0.137\mu_2(2)\mu_2^2(6)\mu_2(8) \\ - 0.855\mu_2(2)\mu_2(6)\mu_2^2(8), \end{aligned} \tag{4.27a}$$

with

$$r = \sqrt{2}\left[\sum_{\sigma}\sigma^{1/2}\mu_2^2(\sigma)\right]\Big/\left[\sum_{\sigma}\sigma\mu_2^2(\sigma)\right]. \tag{4.27b}$$

We next turn to *bcc* O^8. From Table III, we see that the four $m = 2$ states $\sigma = 2$, 4, 6, and 8 are all allowed. We set our coordinate

frame origin on the threefold axis [111], at its intersection with the twofold axis [110], [011], and [101]. (This is the point $(\frac{1}{8}\ \frac{1}{8}\ \frac{1}{8})$ of the O^8 unit cell, with point-group symmetry (32).) In this case, the phases $\psi_2(h,k,l)$ are[2]

$$\psi_2(110) = -\psi_2(\bar{1}10) - \pi/2 = 0 \text{ or } \pi.$$

$$\psi_2(200) = -\pi/2 \text{ or } +\pi/2,$$

$$\psi_2(112) = \psi_2(\bar{1}\bar{1}2) = -\psi_2(1\bar{1}2) - \pi/2 = 0 \text{ or } \pi,$$

$$\psi_2(220) = \psi_2(\bar{2}20) + \pi = 0 \text{ or } \pi. \tag{4.28}$$

All other phases may be obtained from the above by cyclic permutation of the (h,k,l) indices. Note that this space group symmetry corresponds to $p = 1$ in Eqs. (4.16) and (4.23).

Choosing in each case the *first-mentioned allowed value for the phase angle*, the third- and fourth-order terms in (3.13) were computed using the technique discussed previously. The result for f is[2]

$$\begin{aligned} f_{O^8} = \frac{1}{4}\sum_{\sigma}[t - \kappa^2 + \kappa^2(\sigma^{1/2}r/\sqrt{2} - 1)^2]\mu_2^2(\sigma) - 0.625\mu_2^3(2) \\ - 0.422\mu_2^3(6) \\ + 1.016\mu_2^3(8) - 2.186\mu_2^2(2)\mu_2(4) - 1.306\mu_2^2(2)\mu_2(6) \\ - 3.091\mu_2^2(4)\mu_2(8) \\ + 0.880\mu_2^2(6)\mu_2(8) + 0.101\mu_2(2)\mu_2^2(6) + 2.147\mu_2(4)\mu_2^2(6) \\ + 3.039\mu_2(2)\mu_2(4)\mu_2(6) - 2.639\mu_2(2)\mu_2(6)\mu_2(8) \\ + 1.169\mu_2^4(2) + 1.083\mu_2^4(4) \\ + 1.313\mu_2^4(6) + 1.299\mu_2^4(8) + 1.001\mu_2^3(2)\mu_2(4) \\ - 0.342\mu_2^3(2)\mu_2(6) \\ + 0.530\mu_2^3(2)\mu_2(8) + 0.976\mu_2^3(6)\mu_2(8) + 0.554\mu_2(2)\mu_2^3(6) \end{aligned}$$

$$
\begin{aligned}
&- 0.982\mu_2(4)\mu_2^3(6) \\
&+ 3.499\mu_2^2(2)\mu_2^2(4) + 2.291\mu_2^2(2)\mu_2^2(6) + 2.714\mu_2^2(2)\mu_2^2(8) \\
&+ 3.281\mu_2^2(4)\mu_2^2(6) \\
&+ 2.542\mu_2^2(4)\mu_2^2(8) + 4.273\mu_2^2(6)\mu_2^2(8) - 0.144\mu_2^2(2)\mu_2(4)\mu_2(6) \\
&+ 1.717\mu_2^2(2)\mu_2(4)\mu_2(8) - 1.039\mu_2^2(2)\mu_2(6)\mu_2(8) \\
&+ 1.734\mu_2(2)\mu_2^2(4)\mu_2(6) \\
&- 2.165\mu_2(2)\mu_2(4)\mu_2^2(6) + 1.381\mu_2(2)\mu_2^2(6)\mu_2(8) \\
&- 1.729\mu_2(2)\mu_2(6)\mu_2^2(8) \\
&- 2.968\mu_2(4)\mu_2^2(6)\mu_2(8) - 2.473\mu_2(2)\mu_2(4)\mu_2(6)\mu_2(8), \quad (4.29)
\end{aligned}
$$

with r given by Eq. (4.27*b*) (now, of course, the sum is on $\sigma = 2$, 4, 6, and 8).

Consider finally the *sc* group O^2. This structure results from a different modification of the basic tetrahedral skeleton analyzed earlier. We introduce a *sub-harmonic*, whose spatial Fourier components are associated with wave vectors of reduced magnitude q. These wave vectors belong to the set $\langle 100 \rangle$ with $m = 2$ and their local axis systems are given in Table IV. It is clear that these Fourier components destroy *bcc* translational invariance; the resulting structure is *sc*.

For all simple cubic groups the four lowest-lying states have $\sigma = 1$, 2, 3 and 4. For O^2, however, the $m = 2$, $\sigma = 3$ and 4 harmonics are *forbidden*. Thus only two amplitudes need be considered explicitly. The phases are fixed by setting the origin of the coordinate

TABLE IV

Wave vectors and local axis systems $(\hat{\xi},\hat{\eta},\hat{\xi})$ for $\langle 100 \rangle$ wave vectors. For the wave vectors $-\boldsymbol{\kappa}_{1,n}$, $\hat{\eta}_{1,n}$ is replaced by $-\hat{\eta}_{1,n}$. The wave vector parameter q is determined, in general, from Eq. (3.11).

Wave vector ($\boldsymbol{\kappa}_{1,n} = q\hat{\xi}_{1,n}$)	$\hat{\xi}_{1,n}$	$\hat{\eta}_{1,n}$
$\boldsymbol{\kappa}_{1,1} = q\hat{x}$	$\hat{y}$	$\hat{z}$
$\boldsymbol{\kappa}_{1,2} = q\hat{y}$	$\hat{z}$	$\hat{x}$
$\boldsymbol{\kappa}_{1,3} = q\hat{z}$	$\hat{x}$	$\hat{y}$

frame at the point (000) in the O^2 unit cell with point-group symmetry 23. It is easy to see that, for the order parameter being considered, the free energy is *independent* of $\psi_2(1,n)$ and that the appropriate choice for the $\psi_2(2,n)$ is $p = 0$. The result is[2]

$$f_{O^2} = \frac{1}{4}[t - \kappa^2 + \kappa^2(r/\sqrt{2} - 1)^2]\mu_2^2(1) + \frac{1}{4}[t - \kappa^2 + \kappa^2(r - 1)^2]\mu_2^2(2)$$

$$- 3.091\mu_2^2(1)\mu_2(2) + 1.016\mu_2^3(2) + 1.083\mu_2^4(1) + 2.542\mu_2^2(1)\mu_2^2(2)$$

$$+ 1.299\mu_2^4(2), \quad (4.30a)$$

with, from Eqs. (3.11) and (3.12)

$$r = \sqrt{2}[\mu_2^2(1) + \sqrt{2}\mu_2^2(2)]/[\mu_2^2(1) + 2\mu_2^2(2)]. \quad (4.30b)$$

The free energy of the usual cholesteric (helicoidal) phase was given earlier in Eq. (4.5).

We now determine which of the five phases (I,C,O^2,O^5,O^8) is the thermodynamically stable one at any point in the chirality-temperature plane. This is done by minimizing the free energy functionals in Eqs. (4.5), (4.27), (4.29) and (4.30) and then choosing that structure whose f_{min} (assumed negative, otherwise I is the stable phase) is lowest. For O^8, in particular, there are *three* local minima in the parameter space $\{\mu_2(\sigma)\}$ and care must be taken to find the global minimum for this structure.[2]

The resulting phase diagram is shown in Figure 5(b). It contains five phases; in particular, O^5, O^2, and O_c^8 structures appear in the BP region. The O_c^8 structure differs from the two other possible phases with O^8 structure, in that the $\sigma = 2$ phases in Eq. (4.28) are given by[1,2]

$$\psi_2(110) = -\psi_2(\bar{1}10) - \pi/2 = \pi. \quad (4.31)$$

This is equivalent to replacing $\mu_2(2)$ by its negative in Eq. (4.29).

Note that the free energy differences between the various cubic structures (including those O^8 structures not appearing in Figure 5(b)) is small. Thus neglected terms in the Landau free energy density, while negligible in other respects (*e.g*, Bragg peak intensities, latent heats, NMR spectra), could have a significant effect on the phase diagram. In fact, experimental data for BPI and BPII are, in general, in good agreement with the structure assignments *BPI* $\leftrightarrow$ O_c^8; *BPII*

$\leftrightarrow O^2$. However, it is clear that BPIII does *not* have the cubic O^5 structure; here other possibilities must be considered.

D. Non-Cubic Structures

All the cubic phases discussed above take a tetrahedral "skeleton" (see Figure 4) as their starting point. However, several authors have pointed out that interesting *non-cubic* structures are obtained when a skeleton formed by a regular *icosahedron* of wave vectors[18] is considered. This has, in fact, been the basis of suggested *quasicrystalline* structures for BPIII.[15-17]

Since an extensive review on the theory of icosahedral liquid crystal structures has recently been given,[22] we shall not go into the analysis of such structures here. In general, it was found that when a small number of wave vector magnitudes (two or three) were included in the icosahedral order parameter, the resulting free energy is slightly *higher* than that of the O^5 cubic structure. However, as already stressed, Landau free energy calculations can only be regarded as indicative of possible structures for the experimentally observed phases. Thus the possibility that BPIII is characterized by an icosahedral structure certainly deserves further study.

V. SUMMARY

A detailed comparison of the Landau model predictions with experimental results have been given elsewhere.[2] We shall therefore refer here briefly only to the basic experimental properties noted in Section II.

(1) As is evident from Figure 5, the BP eventually disappears when the cholesteric pitch is increased, in agreement with experiment.

(2) As the reduced unit of temperature (t) is of the order of 1 K, the BP region is indeed a narrow one in the physically relevant region ($\kappa \simeq 1$).[2]

(3) It is theoretically possible to have more than one BP structure, in agreement with experiment.

(4) All the theoretical BP structures will exhibit strong optical activity. Since they are cubic, there can be no birefringence.

(5) The theoretical BP structures are characterized by well-defined Fourier components; thus these phases will exhibit Bragg scattering. The predicted scattering peak positions and amplitudes are in good agreement with most experimental results.[2]

(6) For BPIII, an icosahedral structure has been suggested on the basis of a Landau theory analysis.[15-17] While experimental results to date do not confirm this structure, they do not rule it out either.[15,22]

(7) The latent heats between any two of the theoretical BP structures is small compared with that between any one of them and the disordered phase,[2] in agreement with experiment.

(8) Using the Landau model, it is possible, in principle, to calculate interface energies between a BP and the disordered phase. Crystallite shapes could then be calculated theoretically and compared with experiment. This has not yet been done.

(9) Free energy calculations in the presence of an external field can also be carried out straightforwardly using the techniques outlined in Section IV. Initial results along these lines have been encouraging; both with regard to crystallite orientation in a weak field[23] and the prediction of new structures above threshold field values.[4,13]

We conclude by noting several unresolved questions where further theoretical analysis could be useful. One of central importance is the nature of BPIII. Here further analysis of the properties of the icosahedral structure could help; as a start, the theoretical NMR spectrum has been calculated.[24,25]

A second question is the applicability of the selection rules (see Table III) to multiple scattering processes. This point arose following the apparent observation by Tanimoto and Crooker[26] of a polarization-dependent [111] reflection in BPII. Since Bragg scattering in cholesterics is strong rather than weak, it is possible than kinematical scattering models[3,20] are not sufficient and that dynamical scattering theory must be used. Some studies have been carried out along these lines[27] but a complete analysis including, in particular, multiple scattering processes, is still lacking.

Finally, we note the existence of the thermodynamically stable noncubic (one tetragonal and two hexagonal[5,6]) BP in external fields. An early Landau theory analysis[4] indeed predicted the existence of one of the hexagonal structures later observed.[5] Further calculations[13] have confirmed that a second hexagonal phase should exist; the tetragonal BP requires additional analysis.

Acknowledgments

We have benefited from discussions with many colleagues and co-workers over the past decade. Our work has been supported in part by grants from the United States-Israel Binational Science Foundation (BSF) and the Israeli Academy of Arts and Sciences, both in Jerusalem, Israel.

References

1. H. Grebel, R. M. Hornreich and S. Shtrikman, *Phys. Rev.*, **A28**, 1114 (1983).
2. H. Grebel, R. M. Hornreich and S. Shtrikman, *Phys. Rev.*, **A30**, 3264 (1984).
3. A theoretical review has been given by: V. A. Belyakov and V. E. Dmitrienko, *Usp. Fiz. Nauk.*, **146**, 369 (1985); trans.: *Sov. Phys. Usp.*, **28**, 535 (1985).
4. R. M. Hornreich, M. Kugler and S. Shtrikman, *Phys. Rev. Lett.*, **54**, 2099 (1985).
5. P. E. Cladis, T. Garel and P. Pieranski, *Phys. Rev. Lett.*, **57**, 2841 (1986).
6. A recent experimental review has been given by: H. Stegemeyer, Th. Blümel, K. Hiltrop, H. Onusseit and H. Porsch, *Liq. Cryst.*, **1**, 3 (1986).
7. D. K. Yang and P. P. Crooker, *Phys. Rev.*, **A35**, 4419 (1987).
8. E. I. Demikhov, V. K. Dolganov and S. P. Krylova, *Pisma Zh. Eksp. Teor. Fiz.*, **42**, 15 (1985); trans.: *JETP Lett.*, **42**, 16 (1985).
9. R. N. Kleinman, D. J. Bishop, R. Pindak and P. Taborek, *Phys. Rev. Lett.*, **53**, 2137 (1984); J. Thoen, *Phys. Rev. A*, in press.
10. P. Pieranski, R. Barbet-Massin and P. E. Cladis, *Phys. Rev.*, **A31**, 3912 (1985).
11. L. D. Landau and E. M. Lifshitz, *Statistical Physics* (Pergamon Press, Oxford, 1980), Chap. 14.
12. P. G. de Gennes, *The Physics of Liquid Crystals* (Clarendon Press, Oxford, 1975).
13. R. M. Hornreich and S. Shtrikman, *Twelfth Intern. Liq. Cryst. Conf.*, Aug. 1988 and to be published.
14. R. M. Hornreich and S. Shtrikman, *J. Phys. (Paris)*, **41**, 335 (1980); **42**, 367 (1981) (E).
15. R. M. Hornreich and S. Shtrikman, *Phys. Rev. Lett.*, **56**, 1723 (1986).
16. D. S. Rokhsar and J. P. Sethna, *Phys. Rev. Lett.*, **56**, 1727 (1986).
17. V. M. Filev, *Pisma Zh. Eksp. Teor. Fiz*, **43**, 523 (1986); trans.: *JETP Lett.* **43**, 677 (1986).
18. H. Kleinart and K. Maki, *Fortschr. Phys.*, **29**, 219 (1981).
19. R. M. Hornreich and S. Shtrikman, *Phys. Rev.*, **A24**, 635 (1981).
20. R. M. Hornreich and S. Shtrikman, *Phys. Lett.*, **82A**, 345 (1981); Ibid, *Phys Rev.* **A28**, 1791, 3669(E) (1983).
21. R. M. Hornreich and S. Shtrikman, *Z. Physik*, **B68**, 369 (1987).
22. R. M. Hornreich, to be published in *Aperiodic Crystals*, edited by M. Jaric (Academic Press, NY) Vol. II.
23. D. Lubin and R. M. Hornreich, *Phys. Rev.*, **A36**, 849 (1987).
24. R. M. Hornreich and S. Shtrikman, *Phys. Rev. Lett.*, **59**, 68 (1987).
25. V. M. Filev, *Pisma Zh. Eksp. Teor. Fiz.*, **45**, 190 (1987); trans.: *JETP Lett.*, **45**, 235 (1987).
26. K. Tanimoto and P. P. Crooker, *Phys. Rev.*, **A29**, 1566 (1984).
27. V. A. Belyakov, V. E. Dmitrienko and S. M. Osadchii, *Zh. Eksp. Teor. Fiz.*, **83**, 585 (1982); trans.: *Sov. Phys. JETP*, **56**, 322 (1982).